Chemistry Europe
European Chemical Societies Publishing

WILEY VCH

Excellence in Chemistry Research

Announcing our new flagship journal

- Gold Open Access
- Publishing charges waived
- Preprints welcome
- Edited by active scientists

Meet the Editors of *ChemistryEurope*

Luisa De Cola
Università degli Studi di Milano Statale, Italy

Ive Hermans
University of Wisconsin-Madison, USA

Ken Tanaka
Tokyo Institute of Technology, Japan

Chemistry–A European Journal
Research Article
doi.org/10.1002/chem.202202860
Chemistry Europe
European Chemical Societies Publishing
www.chemeurj.org

The Transformation of Inorganic to Organic Carbonates: Chasing for Reaction Pathways in Mechanochemistry

Miriam Sander,[a] Sven Fabig,[a] and Lars Borchardt*[a]

Abstract: Mechanochemical reactions are solvent-free alternatives to solution-based syntheses enabling even conventionally impossible transformations. Their reaction pathways, however, usually remain unexplored within the heavily vibrating, dense milling vessels. Here, we showcase how the green organic solvent diethyl carbonate is synthesized mechanochemically from inorganic alkali carbonates and how the complementary combination of milling parameter studies, synchrotron X-ray diffraction real time monitoring, and quantum chemical calculations reveal the underlying reaction pathways. With this, reaction intermediates are identified, and chemical concepts of solution-chemistry are challenged or corroborated for mechanochemistry.

Introduction

Mechanochemistry has attracted great attention as environmentally-benign alternative via solvent-free reactions and is considered one of the 10 world-changing technologies.[1] Due to its plethora of advantages, the priority is to further expand mechanochemical approaches into chemistry across all fields and real-world applications.[2,3] However, the mechanistic understanding of mechanochemical processes is commonly limited, since the milling is conducted in closed dense devices.[4] Conventional *ex situ* analysis does not depict the state of the system under the reaction conditions and transformations cannot be captured.[5,6] Indeed, by time-resolved *in situ* monitoring, for example, based on powder X-ray diffraction (pXRD) or Raman spectroscopy it is possible to bridge this gap and to track reactions.[7] Yet, the former method is limited to crystalline materials and the latter has restrictive requirement towards the applied reaction setup (e.g., translucence) rendering the elucidation of reaction mechanisms challenging particularly for small liquid organic molecules.[5,8] To overcome this limitation, we pursue the idea of applying quantum chemical calculations in addition.

The overall goal of our work is therefore to find a procedure to clarify underlying mechanisms and intermediates in mechanochemical reactions, which can only be achieved by the complementary combination of parameter variation, *in situ* monitoring, and quantum chemical calculations as shown in former work.[9] As target system, we chose the formation of an organic dialkyl carbonate from inorganic carbonates via a reaction pathway, which is only realizable by mechanochemistry according to Mack et al.[10] The linear forms of dialkyl carbonates, such as diethyl carbonate (DEC), are classified as green chemicals due to low toxicity and high biodegradability.[11] Due to their reaction behavior, polarity as well as excellent solubility, they are used as building blocks for organic synthesis, in pharmaceuticals and for lithium-ion batteries.[12,13] The most common synthesis of dialkyl carbonates starts with a carbonyl source, such as CO_2 or metal carbonates, and the addition of alkyl substituents. Thereby, the synthesis in solution suffers from the incompatibility of solubility and reactivity of the alkyl substituent and the metal carbonate dissolved in the same solvent.[12,14] In this contribution, we present the first formation of DEC via an alkylation reaction of alkali carbonates applying a solvent-free mechanochemical approach (Figure 1), that overcomes solubility limitations and enables this formerly impossible reaction. An in-depth study on reactants, milling intensity, and mechanical force combined with synchrotron pXRD real-time reaction monitoring as well as quantum chemical calculations of the different reaction pathways towards product and side products allowed us to mechanistically elucidate and predict the outcome of such mechanochemical reactions.

Results and Discussion

Mechanochemical alkylation reaction

The target reaction of alkali carbonates with the alkylating agent ethyl trifluoromethanesulfonate (ethyl triflate, EtOTf) was chosen, which can be classified to proceed according to a common S_N2 mechanism. Firstly, the influence of the Hard-Soft-Acid-Base (HSAB) concept in mechanochemistry is examined by

[a] *M. Sander, Dr. S. Fabig, Prof. Dr. L. Borchardt*
Inorganic Chemistry I
Ruhr-Universität Bochum
Universitätsstraße 150, 44801 Bochum (Germany)
E-mail: lars.borchardt@rub.de
Homepage: https://www.borchardt-group.com

Supporting information for this article is available on the WWW under https://doi.org/10.1002/chem.202202860

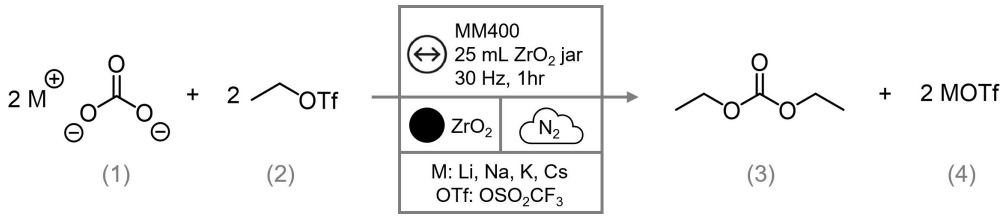

Figure 1. Reaction scheme for the mechanochemical reaction of alkali carbonates (1) with an alkylating agent (2) to diethyl carbonate (3) and the corresponding salt (4).

the variation of the reactants. Therefore, the alkali carbonates of lithium, sodium, potassium, and caesium were used with EtOTf in a stoichiometric approach under moderate milling conditions (ZrO_2, 30 Hz, 60 min) in a mixer mill (Figure 2). For all used alkali carbonates DEC was produced and the according triflate salts

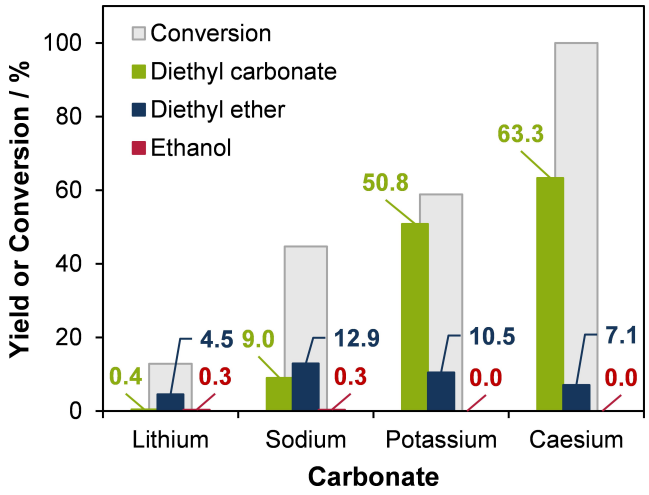

Figure 2. Yield of diethyl carbonate (DEC), diethyl ether and ethanol as well as conversion of ethyl trifluoromethanesulfonate (EtOTf) after the mechanochemical alkylation reaction of varying carbonates (8 mmol) with EtOTf (16 mmol). The milling was carried out by using the MM400 at 30 Hz for 60 min with a 25 mL ZrO_2 vessel and eight ZrO_2 milling balls (d = 10 mm). Determination via calibration of ^{1}H-NMR spectroscopy on DEC. Please note, the deviations between the conversion of EtOTf and the sum of all yielded products can be based on the reaction with traces of water to the according triflic acid, and the decomposition of DEC or EtOTf.

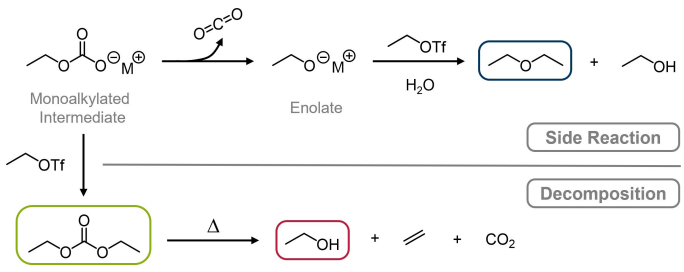

Figure 3. Reaction scheme for the side reaction to diethyl ether and ethanol due to the decarboxylation of the monoalkylated intermediate to the alkoxide (M: alkali metal, OTf: OSO_2CF_3). Assumed decomposition reaction of diethyl carbonate during the milling, which generates ethanol, ethylene, and CO_2.

were validated via pXRD pattern (Figure S1 in Supporting Information) and IR spectra (Figure S2). The formation of the side product diethyl ether results from the decarboxylation of the monoalkylated carbonate salt as intermediate to yield an alkoxide, which displaces the carbonate. Traces of water inside the system cause the formation of ethanol (Figure 3).[10,14] Furthermore, the alcohol can be caused by the decomposition of DEC (see Supporting Information section 2). This illustrates that the milling time must be set precisely for the actual alkylation reaction to DEC – long enough for a sufficient conversion but without decomposing a significant part of the product.

Moreover, there is a distinct trend with the alkali metals that has a large effect on the efficiency of the reaction. Firstly, both the yield of DEC as well as the conversion of EtOTf tend to increase with a lower charge density of the alkali metal ion. Secondly, with a higher charge density of the metal ion the yield of ether is relatively higher compared to the yield of DEC. Here, with lithium carbonate diethyl ether represents the main product, in contrast to the most effective reaction with caesium carbonate showing a high yield of DEC with 63% and a comparatively low part of ether. According to the HSAB concept Li^+, Na^+ and K^+ cations are classified as hard acids, whereas the Cs^+ is a soft acid.[15] The CO_3^{2-} anion is a hard base and the OTf^- anion as leaving group represents a soft base.[15,16] The metal-oxygen interaction in the carbonate and the interplay between metal ion and triflate ion are the two main interactions, which drive the ball milling reaction.[10,17] On the one hand, the weaker the metal ion is bound to the carbonate, the more likely it will coordinate to the triflate ion, which enables the reaction as leaving group. On the other hand, if a strong metal-triflate ion pair is formed, it will be preferably produced. The lithium ion as hard acid is more likely paired with the carbonate ion as hard base than with the triflate ion, whereas the caesium ion as soft acid prefers the interaction with the triflate ion, which increases the yield of DEC and the conversion of EtOTf. Accordingly, the stronger metal-oxygen bounds in the intermediate, the more preferred is the decarboxylation compared to the intended second alkylation reaction. Following the HSAB concept, one would assume that with lithium carbonate no alkylation reaction would take place at all. Nevertheless, it is mechanochemically enabled (see Supporting Information section 2). Rubidium carbonate was only included for the quantum chemical calculations since the trend was already experimentally apparent.

Influence of milling parameters

Since the mechanochemical reaction between K_2CO_3 and EtOTf at 30 Hz for 60 min with ZrO_2 as milling media showed a moderate DEC yield of about 50% (Table 1, Entry 1), respectively a conversion of 60%, it was used as standard reaction to investigate the influence of various milling and chemical parameters. Therefore, only the evaluated parameter was changed (Table 1).

The reaction time is, like in solvent-based chemistry, also for mechanochemical syntheses one of the simplest options to control the energy input during the process. The quantification (Table 1, Entry 2–6) shows the distinct trend that with a longer milling time the conversion as well as the yield of DEC and Et_2O increased until 90 min. By a longer milling time the carbonate is grounded finer, which benefits the reaction process.[17] Moreover, the decarboxylation of the intermediate is favored by the expanded milling time as the yield of the ether increases relatively more than those of DEC. After 90 min, the yield of DEC counted 64%, 14% of ether and 2% of ethanol with a conversion of 93%. By further expansion of the milling time up to 120 min, the yield of DEC was almost consistent, whereas the amount of ether developed. This indicates that with a higher milling time of 120 min the decomposition reaction of DEC must have a significant influence. Thereby, EtOH is developed, which can further react with EtOTf to ether. Thinking of yield and industrial costs, a higher reaction time than 90 min has no benefits. The parameter milling frequency has a direct impact

Table 1. Investigation of the reaction parameters of the mechanochemical alkylation reaction. Parameters if not stated otherwise: K_2CO_3 (8 mmol) and ethyl trifluoromethanesulfonate EtOTf (16 mmol) were milled for 60 min at a milling frequency of 30 Hz with ZrO_2 as vessel and milling ball material. The milling was carried out in the MM400 mixer mill with a 25 mL milling vessel and a quantity of eight milling balls (d = 10 mm) under N_2 atmosphere. Yield of diethyl carbonate (DEC), diethyl ether (Et_2O) and ethanol (EtOH) as well as the conversion of the alkylating agent (EtOTf) after the mechanochemical alkylation reaction. Please note, the deviations between the conversion of EtOTf and the sum of all yielded products can be based on the reaction with traces of water to the according triflic acid, and the decomposition of DEC or EtOTf.

Entry	Evaluated Parameter	Yield DEC[a] [%]	Yield Et_2O[b] [%]	Yield EtOH[b] [%]	Conversion EtOTf[c] [%]
1	–	50.8	10.5	0.0	58.8
Milling time					
2	10 min	12.9	1.3	0.3	31.2
3	30 min	32.4	5.4	0.0	53.1
4	60 min	50.8	10.5	0.0	58.8
5	90 min	63.5	14.1	1.9	92.9
6	120 min	64.8	26.3	4.4	94.0
Milling frequency					
7	0 Hz	0.3	0.3	0.2	n.sp.[d]
8	10 Hz	11.3	1.8	0.6	24.4
9	25 Hz	47.3	6.6	0.7	54.2
10	30 Hz	50.8	10.5	0.0	58.8
11	35 Hz	59.6	23.5	3.1	93.6
Milling material					
12	Teflon	21.7	4.3	0.3	46.3
13	Zirconium dioxide	50.8	10.5	0.0	58.8
14	Stainless steel	57.5	5.8	0.9	83.5
Additives[e]					
15	AcN (100 µL)	58.2	8.7	2.2	99.2
16	DMSO (100 µL)	9.0	28.1	1.6	93.2
17	DMF (100 µL)	16.1	2.0	1.3	81.9
18	18-crown-6 (16 mmol)	6.2	27.6	n.sp.[d]	100.0
19	CO_2 (0.2 g)[f]	74.1	0.7	0.0	100.0
Optimized/Best Parameters					
20	K_2CO_3, optimized[g]	71.1	1.6	0.0	100.0
21	Cs_2CO_3, optimized[g]	68.3	0.8	0.0	100.0
22	K_2CO_3, best[h]	73.5	1.1	0.0	100.0
23	Cs_2CO_3, best[h]	84.6	1.1	1.1	100.0

[a] Determined via ^{1}H NMR spectroscopy, analysis with calibration of DEC in $CDCl_3$ at 300 MHz, based on the limiting species; [b] Determined via ^{1}H NMR spectroscopy, analysis based on the amount of DEC and the ratio of integrals, based on the input of EtOTf and the considered side reaction; [c] Determined via ^{1}H NMR spectroscopy, based on the amount of DEC and the ratio of integrals, based on the input of EtOTf; [d] not specified (n.sp.); [e] See Supporting Information section 3; [f] One equivalent excess of potassium carbonate (12.5 mmol) compared to stoichiometric reaction; [g] The milling was carried out at 30 Hz for 90 min with a 25 mL st. steel vessel and milling balls, compared to the stoichiometric reaction the carbonates were used with 1 equiv. excess but the total mass was kept equal; [h] The milling was carried out at 30 Hz for 60 min with a 25 mL ZrO_2 vessel and milling balls, compared to the stoichiometric reaction the carbonates were used with 1 equiv. excess but the total mass was kept equal.

on the kinetic energy of the grinding media and commonly increases the conversion but limits the selectivity.[3,19] The mechanochemical alkylation was carried out for 60 min at varying milling frequencies (Table 1, Entry 7–11), whereby 0 Hz illustrates that the reactants were only mixed without grinding. It was demonstrated that without mechanochemical impact the yield of DEC and side products with 0.3% each is neglectable. Additionally, it clarifies that the mechanochemical force does not cause the development of side products. With a higher milling frequency, the conversion increased, just like the yield of DEC and the side products. Until the frequency of 30 Hz the amount of DEC and the side products extended in almost the same ratio. Reaching the 35 Hz, the amount of diethyl ether doubled compared to the 30 Hz, which corresponds to an increase in the ratio of ether to DEC from 20% to 40%. Nevertheless, a higher kinetic energy benefits this mechanochemical reaction, but it must be set precisely. For the varied milling media, the material density increases from Teflon over ZrO_2 to stainless (st.) steel (Table 1, Entry 12–14).[20] The conversion of EtOTf as well as the yield of DEC increased steadily with a higher material density since the energy of a moving body is proportional to its mass. To summarize, by optimizing the milling parameters, the conversion as well as the yield of DEC can be increased. Thereby, it must be considered that the decomposition of DEC takes place more frequently with a higher energy impact. Moreover, the decarboxylation can be unintentionally favored, which will be validated by quantum chemical calculations.

Consequently, we tried to accelerate the mechanochemical alkylation through its chemical parameters by adding traces of polar, aprotic solvents (Table 1, Entry 15–17) to facilitate the considered S_N2 mechanism via liquid-assisted grinding. Neither for the addition of acetonitrile (AcN) nor of dimethyl sulfoxide (DMSO) and of dimethylformamide (DMF) the desired effect occurred, but rather the results were adversely affected by side reactions (see Supporting Information section 3). Furthermore, 18-crown-6 ether (Table 1, Entry 18) was added to increase the nucleophilicity of the carbonate, whereby only the side reaction to diethyl ether was facilitated.

To investigate the limiting compound of the reaction and the chemical kinetics, the mechanochemical reaction was carried out under moderate conditions (ZrO_2, 30 Hz, 60 min). Thereby, one equivalent (1 equiv.), respectively three equivalents (3 equiv.) of K_2CO_3 and EtOTf were used with an equal total mass compared to the stoichiometric approach (Figure 4). By using 1 equiv. excess of EtOTf the conversion increased by approximately 20% and the yield of ether to the same extent, whereas the yield of DEC remained almost the same. This distinct trend is as well detectable for the 3 equiv. excess, whereby the amount of ether further increased, so that the conversion exceeded the stoichiometrically required amount (> 100%). This clarifies that some of the excess EtOTf must, for example, decompose. Since the yield of DEC is not benefited by an excess of EtOTf, the formation of the monoalkylated intermediate is most likely confirmed. Although the excess of EtOTf induces a faster formation of the intermediate, its decarboxylation is not hindered by the higher quantity of

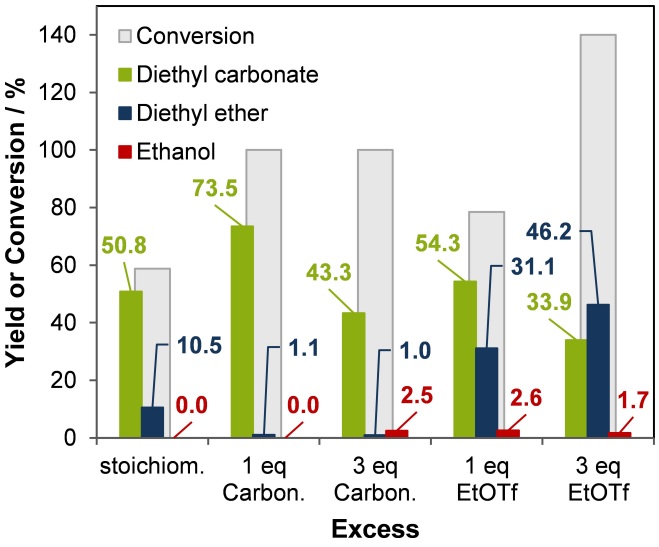

Figure 4. Yield of diethyl carbonate (DEC), diethyl ether and ethanol as well as conversion of ethyl trifluoromethanesulfonate (EtOTf) after the mechanochemical alkylation reaction of K_2CO_3 with EtOTf. In comparison to the stoichiometric (stoichiom.) reaction, a one equivalent (1 equiv.) or three equivalents (3 equiv.) excess of either K_2CO_3 (Carbon.) or EtOTf was used with an equal total mass. The milling was carried out by using the MM400 at 30 Hz for 60 min with a 25 mL ZrO_2 vessel and eight ZrO_2 milling balls (d = 10 mm). Determination via calibration of ^{1}H-NMR spectroscopy on DEC. For the approaches using an excess of EtOTf, the conversion was calculated regarding only the amount of EtOTf, which is necessary for the stoichiometric reaction based on the amount of K_2CO_3. Note, a conversion of more than 100% is only arithmetically possible.

alkylating agent. This means in turn that the amount of alkylating agent cannot accelerate the second S_N2 reaction and does not represent the limiting factor of the reaction. Even a decrease of DEC yield is noticeable for 3 equiv. excess of EtOTf, whereby it is likely caused by the high amount of produced ether, which affects the reactivity of the alkylating agent. With a 1 equiv. excess of K_2CO_3 the yield of DEC increased up to 74%, whereas the amount of ether was at 1%. This result demonstrates that the reaction rate of the mechanochemical approach directly depends on the concentration of the nucleophile. Since the amount of side products decreased as well, an excess of the inorganic carbonate favors the second alkylation of the monoalkylated intermediate instead of its decarboxylation. By further increasing the equivalents of carbonate, the yield of DEC decreased. This might be due to the higher amount of solid and a hindered energy transfer from the milling media to the reactants. Overall, it is worth highlighting that although the milling parameters in mechanochemistry are unique compared to solution chemistry, it still follows known reaction mechanisms.

The previously optimized parameters (st. steel, 30 Hz, 90 min) were combined with a 1 equiv. excess for K_2CO_3 and Cs_2CO_3 (Table 1, Entry 20 and 21). Compared to the excess reactions under standard conditions (ZrO_2, 30 Hz, 60 min), the combination of all improved milling conditions resulted in a decrease in the yield of DEC (Table 1, Entry 22 and 23). The reaction with caesium carbonate is likely completed in a

significantly shorter time frame than the set milling time, so that the energy input for the combined parameters leads to a decomposition of DEC. This illustrates the great influence of the chemical parameters for this mechanochemical alkylation. Consequently, the milling parameters must be set precisely as their energy input must be limited due to the occurring side reactions. All in all, the best results were reached with moderate milling conditions and a 1 equiv. excess of the alkali carbonates. Thereby, the reaction with Cs_2CO_3 achieved the highest DEC yield of 85% with 2% of side products and a full conversion.

Time-resolved *in situ* monitoring

We further tracked the reaction process by synchrotron *in situ* pXRD, whereby caesium carbonate was further used due to its high reactivity. Although the reaction product DEC as well as the side products Et_2O and EtOH form as liquids, the reaction can be monitored due the highly crystalline alkali triflate as solid product as well as the consumption of the alkali carbonate as reactant. At 20 Hz, the first crystalline product is observed after 7 minutes and 10 minutes later the mechanochemical reaction is completed (Figure 5). Moreover, it is demonstrated that without milling no product is formed, which verifies it as mechanochemical reaction. Additionally, it is noticeable that during the reaction process a reflex at 24.9° occurred and increased steadily in intensity up to a maximum around 10 min of milling time. After this maximum, a decrease in intensity took place, so that the reflex cannot be found in the product CsOTf. Due to the occurring side products, the mechanism based on

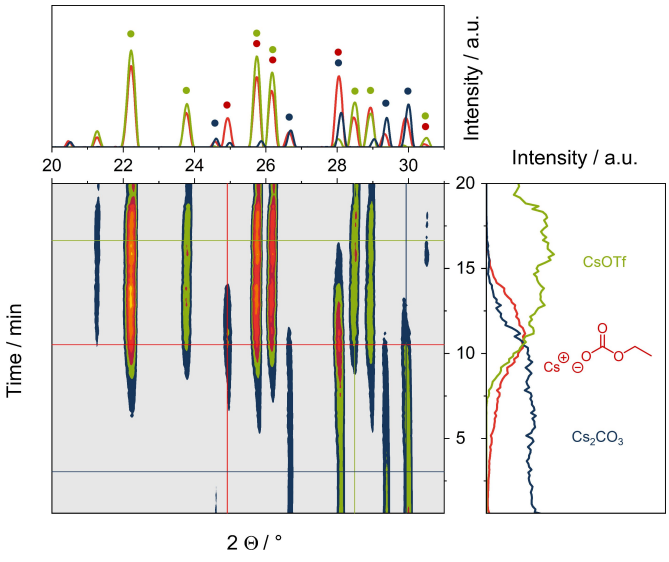

Figure 5. In situ X-ray measurement of the mechanochemical reaction from caesium carbonate with ethyl trifluoromethanesulfonate at a milling frequency of 20 Hz. Presented is the 2D plot based the X ray pattern converted to Cu Kα1 and the signal intensity over time. The caesium carbonate (blue), the caesium triflate (green) as well as the intermediate caesium ethyl carbonate (red) are assigned. The references are assigned by the corresponding-coloured dots and their XRD patterns are shown in the Supplementary (Figure S6).

the formation of the monoalkylated carbonate as intermediate was already proposed. Caesium ethyl carbonate was thus synthesized separately (see Supporting Information section 5) and via pXRD verified as the formed intermediate (Figure S6). Note, that the pattern for the intermediate during *in situ* monitoring contains the patterns of the carbonate and the triflate salt.

To visualize the great influence of the kinetic energy on the reaction course, the reaction was monitored at varying milling frequencies (see Supporting Information section 4). The reaction rate directly depends on the mechanochemical energy input since the onset of the product as well as the end of the reaction were reached faster with a higher frequency, respectively the reverse for lower frequencies. In turn, by utilizing higher frequencies the intermediate can be discovered but its maximum intensity occurs already after 5 min, which indicates that the higher kinetic energy facilitates both consecutive S_N2 reactions, respectively the side reaction.

Quantum chemical calculations

To provide an insight into the mechanism of the reaction and to understand the formation of the side products diethyl ether and ethanol quantum chemical calculations were conducted. We expect the reaction to start with some sort of coordination complex **1** (Figure 6) of the ethyl trifluoromethanesulfonate (shaded part of 1) and the alkali carbonate (non-shaded part of 1). Within this complex **1**, three reaction pathways as depicted by the arrows (green, red, Figure 6) are conceivable with an oxygen atom of the carbonate group acting as a nucleophile in each reaction pathway. As we will demonstrate in this section, the first nucleophilic attack has a crucial effect on the formation of the side products diethyl ether and ethanol. Please take in mind that the oxygen atoms **II** and **III** in **1** are equivalent due to the rotation around the axis between the oxygen atom **I** and the carbon atom in the carbonate. Therefore, only the nucleophilic attacks of **I** and **II** are discussed in the following.

Figure 6 lists the ΔG values for the formation of the products **3I** and **3II** via the transition states **2I** and **2II**. For the lithium containing complex **1-Li** ΔG for the nucleophilic attack of oxygen atom **I** has a value of 19.44 kcal/mol (**2I-Li**), whereas the ΔG value for the nucleophilic attack of **II** amounts to 22.40 kcal/mol (**2II-Li**). Accordingly, for lithium carbonate the formation of **3I-Li** is favoured. In contrast, for the caesium containing complex **1-Cs** the order of the ΔG values for the nucleophilic attack of **I** and **II** is flipped (21.79 kcal/mol for **I** and 18.06 kcal/mol for **II**) and thus the intermediate **3II-Cs** is mainly formed. As a conclusion, the alkali metal in the carbonate directs the nucleophilic attack towards two possible intermediates, namely **3I** and **3II**.

The formation of the intermediates **3I** and **3II** has a substantial influence on the further reaction process. Due to its variety in the orientation of the metal atoms and the former carbonate group, those products can undergo again different reaction pathways. **3I** (Figure 6, top) will either disaggregate into **5** and **6** or undergo a decarboxylation (**4I**) leading to the

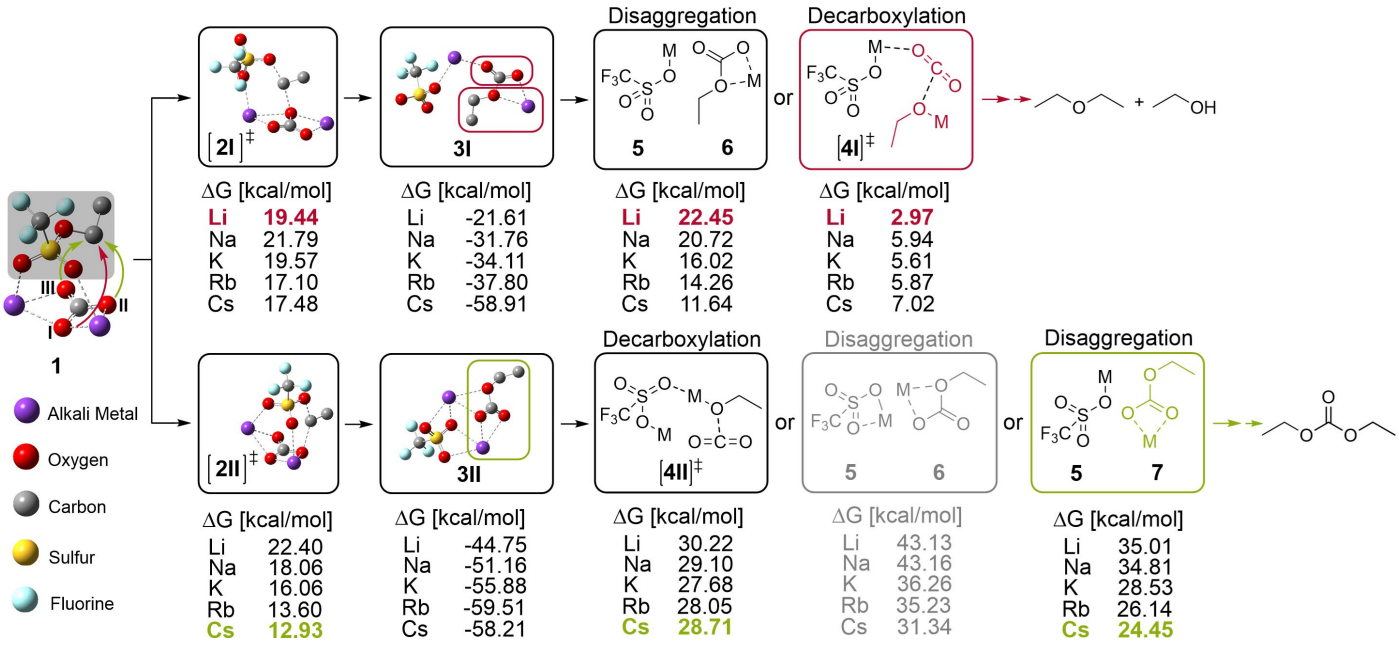

Figure 6. Investigated pathways for the ethylation of alkali carbonates and the labelling system for the reaction. Depicted coordination complexes 1 and 3 as well as the transition states 2 and 4 and the disaggregation products 5, 6 and 7 were either calculated by means of wB97XD or Hartree–Fock with a combination of 6–31G*, 6–31 + G* and def2TZVP basis sets. Exemplarily shown for potassium carbonate.

formation of carbon dioxide and ethanolate. **3II** (Figure 6, bottom) can as well undergo a decarboxylation (**4II**) or disaggregate into **5** and **7** or **5** and **6**, respectively. Since the ΔG values for the decarboxylation of **3I** are much lower than the ΔG values for the disaggregation, **3I** will preferably undergo the decarboxylation, which lead to carbon dioxide and ethanolate and in consequence to the side products diethyl ether and ethanol. On the other hand, for **3II** the decarboxylation is only favoured for the lithium and sodium species, whereas the caesium species will disaggregate into **5** and **7**. Hence, the formation of side products is mainly hindered. The potassium species **3II** can either decarboxylate (27.68 kcal/mol) or form **5** and **7** (28.53 kcal/mol), which is also valid for the rubidium species. Since those values are close to each other and range in the uncertainty of quantum chemical calculations, one can assume a certain formation of carbon dioxide and ethanolate. The structures **6** and **7** can undergo a second ethylation step, which leads to the formation of the desired product diethyl carbonate. For the ΔG values of the second ethylation step as well as a detailed description of the quantum chemical methods and used basis sets see Supporting Information section 6.

Conclusion

In summary, we presented the procedure to reveal the underlying reaction pathways and intermediates of mechanochemical reactions and light up the 'black box'. This was achieved by the complementary combination of *ex situ* analysis after parameter variation, time-resolved *in situ* monitoring and quantum chemical calculations. The mechanochemical alkylation reaction to the green solvent diethyl carbonate starting from inorganic carbonates as target system overcame the issue of reactivity and solubility in this solvent-free approach. By a systematic variation of the chemical as well as the milling parameters two main findings can be declared: Firstly, the used alkali metal directly influences the reaction rate, which proves the validity of the HSAB concept in mechanochemistry. Secondly, a higher energy impact benefits this mechanochemical reaction, but it must be set precisely as the decarboxylation as side reaction and the product decomposition limit the selectivity. The reaction process was successfully tracked via *in situ* pXRD, which further verified the dependency of the reaction rate on the kinetic energy and detected the monoalkylated intermediate. Quantum chemical calculations validated two different pathways for the alkylation reaction as well as the proposed monoethylated intermediate. The first pathway produces the desired diethyl carbonate, whereas during the second pathway carbon dioxide can be easily eliminated. Consequently, the choice of the alkali metal has a tremendous influence on the reaction pathway, which supports the experimental findings. Overall, it becomes clear that no single technique can provide a fundamental understanding of the mechanochemical processes. It is essential to combine experimental and theoretical approaches to unite advantages of individual methods.

Experimental Section

Experimental setup: All reagents and solvents were purchased from commercial suppliers and used without further purification.

The milling was carried out in the *MM400* mixer mill from Retsch with a 25 mL milling vessel and a quantity of eight 10 mm-diameter milling balls under N_2 atmosphere. In a typical synthesis, K_2CO_3 (1.11 g, 8.0 mmol) and ethyl trifluoromethanesulfonate (2.85 g, 16.0 mmol) were milled for 60 min at a milling frequency of 30 Hz with zirconium dioxide as vessel and milling ball material (ball-to-powder ratio of 21.6:1). After the reaction, the vessel was cooled $<0\,^{\circ}C$ for 60 min to keep the evaporating compounds. The crude product was analyzed qualitative and quantitative via ^1H NMR spectroscopy. To obtain the salt as product, the crude mixture was washed with 30 mL dichloromethane, whereby the solution was treated in an ultrasonic bath for 10 min, afterwards centrifugalized and decanted. Varied metal carbonates (8.0 mmol; Li_2CO_3, Na_2CO_3, Cs_2CO_3) were used as well as a milling frequency between 0 Hz and 35 Hz (*MM500* mixer mill from Retsch for 35 Hz), a milling time up to 120 min and HH stainless steel or Teflon as milling material. For an excess of reactants, the total reaction mass was kept equal and the excess of one equivalent, respectively three equivalents, of K_2CO_3 (12.5 mmol; 20.1 mmol) and EtOTf (17.6 mmol; 19.0 mmol) was chosen in comparison to the stoichiometric approach. For milling with additive, the solvents were dried over molsieve and used with a volume of 100 µL. 18-crown-6 ether (4.23 g, 16.0 mmol) was used without additional preparation. Carbon dioxide was added as dry ice (0.2 g), whereby it was prepared under N_2 atmosphere. For the *in situ* X-ray measurement, the *IST636* mixer mill from InSolido Technologies was used with a custom made 19 mL polyfluoroalkoxy (PFA) milling vessel and two 10 mm-diameter ZrO_2 milling balls. Cs_2CO_3 (0.98 g, 3.0 mmol) and ethyl trifluoromethanesulfonate (1.07 g, 6.0 mmol) were milled at a milling frequency of 10 Hz, 20 Hz, 30 Hz and 36 Hz until the reaction was completed.

Characterization: The ^1H NMR spectra were recorded on a Bruker *Avance III HD* spectrometer at 300 MHz in chloroform-d (see Supporting Information section 5). The pXRD measurements were conducted using a LynxEye detector operating at 30 kV acceleration voltage and 10 mA emission current using $Cu_{K\alpha1}$ radiation ($\lambda=$ 1.5406 Å) on the *D2 Phaser* diffractometer from Bruker. The two-dimensional pXRD spectra were collected at the *Desy/Petra III beamline P02.1* using a Perkin Elmer XRD 1621 flat panel detector consisting of an amorphous Si-sensor equipped with a CsI-scintillator (pixel number 2045×2048, pixel size 200×200 µm). The diffractograms were integrated into one-dimensional pXRD patterns with the Dawn Science package using a wavelength $\lambda=$ 0.020733 nm. For creating a two-dimensional figure, the integrated diffractograms were baseline corrected with Sonneveld-Visser algorithm. The FTIR spectroscopy was performed by using the QATR-S ATR unit on the *IRSpirit* from Shimadzu. The measurement was carried out in the wavenumber range of 400–4000 cm^{-1} with 15 scans per measurement of a resolution of 4 cm^{-1}.

Calculations: All calculations were performed with the *Gaussian 16* program package.[21]

Acknowledgements

We gratefully acknowledge the Deutsche Forschungsgemeinschaft DFG for the support of the NISECap project (support code: 4538/7-1). We are grateful to DESY (Hamburg, Germany), a member of the Helmholtz Association HGF, for the provision of experimental facilities. Parts of this research were carried out at Petra III and we would like to thank Dr. Martin Etter for assistance in using beamline P02.1. We further thank Tilo Rensch for performing the pXRD measurements. Open Access funding enabled and organized by Projekt DEAL.

Conflict of Interest

The authors declare no competing interests.

Data Availability Statement

The data that support the findings of this study are available from the corresponding author upon reasonable request.

Keywords: alkali metals · mechanochemistry · nucleophilic substitution · quantum chemical calculations · time-resolved X-ray diffraction

[1] a) F. Gomollon-Bell, *Chem. Int.* **2019**, *41*, 12; b) J.-L. Do, T. Friščić, *Synlett* **2017**, *28*, 2066; c) S. L. James, C. J. Adams, C. Bolm, D. Braga, P. Collier, T. Friščić, F. Grepioni, K. D. M. Harris, G. Hyett, W. Jones, A. Krebs, J. Mack, L. Maini, A. G. Orpen, I. P. Parkin, W. C. Shearouse, J. W. Steed, D. C. Waddell, *Chem. Soc. Rev.* **2012**, *41*, 413.
[2] a) V. Štrukil, M. D. Igrc, M. Eckert-Maksić, T. Friščić, *Chemistry* **2012**, *18*, 8464; b) S. Grätz, L. Borchardt, *RSC Adv.* **2016**, *6*, 64799; c) A. Stolle, B. Ranu, *Ball Milling Towards Green Synthesis: Applications, Projects, Challenges*, Royal Society of Chemistry, Cambridge, **2014**.
[3] A. Stolle, R. Schmidt, K. Jacob, *Faraday Discuss.* **2014**, *170*, 267.
[4] a) S. Mateti, M. Mathesh, Z. Liu, T. Tao, T. Ramireddy, A. M. Glushenkov, W. Yang, Y. I. Chen, *Chem. Commun.* **2021**, *57*, 1080; b) X. Ma, W. Yuan, S. E. J. Bell, S. L. James, *Chem. Commun.* **2014**, *50*, 1585.
[5] A. A. L. Michalchuk, F. Emmerling, *Angew. Chem. Int. Ed.* **2022**, *61*, e202117270.
[6] V. V. Boldyrev, *Russ. Chem. Rev.* **2006**, *75*, 177.
[7] a) T. Friščić, I. Halasz, P. J. Beldon, A. M. Belenguer, F. Adams, S. A. J. Kimber, V. Honkimäki, R. E. Dinnebier, *Nat. Chem.* **2013**, *5*, 66; b) G. I. Lampronti, A. A. L. Michalchuk, P. P. Mazzeo, A. M. Belenguer, J. K. M. Sanders, A. Bacchi, F. Emmerling, *Nat. Commun.* **2021**, *12*, 6134; c) S. Lukin, K. Užarević, I. Halasz, *Nat. Protoc.* **2021**, *16*, 3492.
[8] a) P. A. Julien, K. Užarević, A. D. Katsenis, S. A. J. Kimber, T. Wang, O. K. Farha, Y. Zhang, J. Casaban, L. S. Germann, M. Etter, R. E. Dinnebier, S. L. James, I. Halasz, T. Friščić, *J. Am. Chem. Soc.* **2016**, *138*, 2929; b) M. Leger, J. Guo, B. MacMillan, H. Titi, T. Friscic, B. Blight, B. Balcom, *ChemRxiv.* **2021**; c) P. F. M. de Oliveira, A. A. L. Michalchuk, A. G. Buzanich, R. Bienert, R. M. Torresi, P. H. C. Camargo, F. Emmerling, *Chem. Commun.* **2020**, *56*, 10329; d) F. Puccetti, S. Lukin, K. Užarević, E. Colacino, I. Halasz, C. Bolm, J. G. Hernández, *Chemistry* **2022**, *28*, e202104409.
[9] a) S. Lukin, M. Tireli, I. Lončarić, D. Barišić, P. Šket, D. Vrsaljko, M. Di Michiel, J. Plavec, K. Užarević, I. Halasz, *Chem. Commun.* **2018**, *54*, 13216; b) I. R. Speight, I. Huskić, M. Arhangelskis, H. M. Titi, R. S. Stein, T. P. Hanusa, T. Friščić, *Chem. Eur. J.* **2020**, *26*, 1811; c) T. Rensch, S. Fabig, S. Grätz, L. Borchardt, *ChemSusChem* **2022**, *15*, e202101975.
[10] D. C. Waddell, I. Thiel, A. Bunger, D. Nkata, A. Maloney, T. Clark, B. Smith, J. Mack, *Green Chem.* **2011**, *13*, 3156.
[11] P. G. Jessop, *Green Chem.* **2011**, *13*, 1391.
[12] S. Huang, B. Yan, S. Wang, X. Ma, *Chem. Soc. Rev.* **2015**, *44*, 3079.
[13] a) P. Tundo, L. Rossi, A. Loris, *J. Org. Chem.* **2005**, *70*, 2219; b) B. Schäffner, F. Schäffner, S. P. Verevkin, A. Börner, *Chem. Rev.* **2010**, *110*, 4554; c) A. M. Haregewoin, E. G. Leggesse, J.-C. Jiang, F.-M. Wang, B.-J. Hwang, S. D. Lin, *Electrochim. Acta* **2014**, *136*, 274.
[14] J. A. Cella, S. W. Bacon, *J. Org. Chem.* **1984**, *49*, 1122.
[15] R. G. Pearson, *J. Chem. Educ.* **1968**, *45*, 581.
[16] M. Saito, S. Kawaharasaki, K. Ito, S. Yamada, K. Hayamizu, S. Seki, *RSC Adv.* **2017**, *7*, 14528.
[17] L. N. Ortiz-Trankina, J. Crain, C. Williams, J. Mack, *Green Chem.* **2020**, *22*, 3638.
[18] P. Baláž, *Mechanochemistry in Nanoscience and Minerals Engineering*, Springer, Berlin, Heidelberg, **2008**.

[19] a) C. Suryanarayana, *Prog. Mater. Sci.* **2001**, *46*, 1; b) D. E. Crawford, J. Casaban, *Adv. Mater.* **2016**, *28*, 5747.
[20] https://www.fritsch-international.com/ (accessed July 26, 2022).
[21] M. J. Frisch, G. W. Trucks, H. B. Schlegel, G. E. Scuseria, M. A. Robb, J. R. Cheeseman, G. Scalmani, V. Barone, G. A. Petersson, H. Nakatsuji, X. Li, M. Caricato, A. V. Marenich, J. Bloino, B. G. Janesko, R. Gomperts, B. Mennucci, H. P. Hratchian, J. V. Ortiz, A. F. Izmaylov, J. L. Sonnenberg, Williams, F. Ding, F. Lipparini, F. Egidi, J. Goings, B. Peng, A. Petrone, T. Henderson, D. Ranasinghe, V. G. Zakrzewski, J. Gao, N. Rega, G. Zheng, W. Liang, M. Hada, M. Ehara, K. Toyota, R. Fukuda, J. Hasegawa, M. Ishida, T. Nakajima, Y. Honda, O. Kitao, H. Nakai, T. Vreven, K. Throssell, J. A. Montgomery Jr., J. E. Peralta, F. Ogliaro, M. J. Bearpark, J. J. Heyd, E. N. Brothers, K. N. Kudin, V. N. Staroverov, T. A. Keith, R. Kobayashi, J. Normand, K. Raghavachari, A. P. Rendell, J. C. Burant, S. S. Iyengar, J. Tomasi, M. Cossi, J. M. Millam, M. Klene, C. Adamo, R. Cammi, J. W. Ochterski, R. L. Martin, K. Morokuma, O. Farkas, J. B. Foresman, D. J. Fox, *Gaussian 16 Rev. C.01*, Wallingford, CT, **2016**.

Manuscript received: September 13, 2022
Accepted manuscript online: October 31, 2022
Version of record online: ■■, ■■■

RESEARCH ARTICLE

The synthesis of the green organic solvent diethyl carbonate by mechanochemistry starting from inorganic carbonates is used as target system to light up the 'black box' with its heavily vibrating, dense milling vessels. The complementary combination of milling parameter studies, synchrotron X-ray diffraction real time monitoring, and quantum chemical calculations reveals the underlying reaction pathways and intermediates.

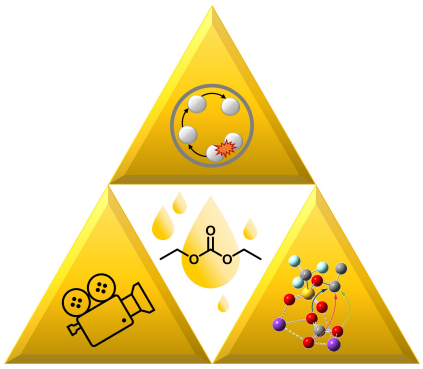

*M. Sander, Dr. S. Fabig, Prof. Dr. L. Borchardt**